Chemical Engineering Journal 319 (2017) 89–97

Contents lists available at ScienceDirect

Chemical Engineering Journal

journal homepage: www.elsevier.com/locate/cej

Fouling in gravity driven Point-of-Use drinking water treatment systems

C. Chawla [a,b], A. Zwijnenburg [a], A.J.B. Kemperman [b,*], K. Nijmeijer [b,1]

[a] Wetsus, European Centre of Excellence for Sustainable Water Technology, Oostergoweg 9, 8911 MA Leeuwarden, The Netherlands

[b] Membrane Science & Technology, MESA+ Institute for Nanotechnology, University of Twente, Faculty of Science and Technology, P.O. Box 217, 7500 AE Enschede, The Netherlands

HIGHLIGHTS

- Fouling in membrane based Point-of-Use drinking water systems was studied.
- Flux stabilization was observed for hollow fiber membrane configuration.
- Two different fouling mechanisms evolved in inside/out vs outside/in configuration.
- Intermittently operated inside/out membrane resulted in lowest hydraulic resistance.

ARTICLE INFO

Article history:
Received 14 November 2016
Received in revised form 20 February 2017
Accepted 22 February 2017
Available online 24 February 2017

Keywords:
Point-of-Use (PoU) systems
Ultrafiltration
Hollow fiber membranes
Biofouling
Intermittent operation

ABSTRACT

This paper describes fouling in simulated Point-of-Use (PoU) systems based on low pressure hollow fiber ultrafiltration membranes. Various operational configurations such as recirculation of feed, discontinuous vs. continuous filtration, and inside/out vs. outside/in were compared to study their effects on fouling and permeate production. Flux values stabilized around 2 L/m^2 h for gravity driven (100 mbar) ultrafiltration. Intermittent operation resulted in lower overall hydraulic resistances compared to continuously operated systems. This was due to the low organic loading and relaxation of the fouling layer during periods of standstill. In most experiments the fouling layer mainly consisted of diatoms, inorganic particles and few microbial clusters. The PoU systems investigated can be operated for longer duration without the need for strong chemical cleaning.

1. Introduction

Lack of potable water remains a major concern for most developing countries. Household Water Treatment (HWT) technologies are increasing in popularity to meet the safe drinking water needs of people. These so-called Point-of-Use (PoU) technologies utilize physical and/or chemical treatment (for surface water and wastewater re-use) to remove contaminants. Physical sieving by membrane filtration is one of the most favorable of all the product technologies due to its robustness in handling different types of feed water and its user friendliness. Membrane technology accounts for the largest market share in manufactured PoU systems [1].

Low pressure ultrafiltration has proven to be an effective technology for potable water production due to its low energy consumption, effective removal of microbes and ease of use [2]. However, fouling still remains a major challenge and adversely affects the water production capacity and operational lifetime of membranes. Major foulants comprise natural organic matter, inorganic elements, and microorganisms present in the feed water, which interact with the membrane surface and attach to it either reversibly or irreversibly. Membrane fouling behavior depends upon various factors such as continuous /intermittent operation [3], membrane configuration/geometries [4] and hydrodynamics [5]. It has been reported that during gravity driven ultrafiltration of surface water, intermittent operation facilitates relaxation of the fouling layer deposited on the membrane surface and leads to increased fluxes [3]. It was also observed that intermittent operation when combined with forward flushing further enhances the performance of the membrane system [3]. On the other hand, fouling was observed to be more severe under continuous operation [3]. In another study, the effect of hollow fiber membrane module design based on 4 different module geometries i.e. straight, helically coiled, twisted and sinusoidal was investigated [4]. It was shown that the mass transfer increased significantly for curved membrane geometries compared to straight ones (as reflected in the correlation between the Dean number (De) and the limiting

* Corresponding author.
E-mail address: a.j.b.kemperman@utwente.nl (A.J.B. Kemperman).

[1] Current address: Membrane Materials and Processes, Eindhoven University of Technology, Department of Chemical Engineering and Chemistry, P.O. Box 513, 5600 MB Eindhoven, The Netherlands.

http://dx.doi.org/10.1016/j.cej.2017.02.120
1385-8947/

permeate fluxes). Yet another study on membrane configuration compared the response of flat sheet modules against hollow fiber membrane modules during treatment of industrial wastewater [6]. It was observed that for similar feed water characteristics, fouling in the flat sheet membrane was dominated by pore blocking as opposed to cake/gel layer formation observed in case of the hollow fiber configuration [6]. The effect of hydrodynamics has also been investigated by employing different feed water flow patterns with respect to the membrane orientation, such as cross-flow and secondary flow. The positive effect of cross-flow velocity on abated fouling has been demonstrated well in literature [5,7–11]. Shamsuddin et al. [5] showed that cross-flow introduced by circular channels, with spirals on the membrane surface, reduced the boundary (fouling) layer thickness on the membranes surface and improved foulant re-dissolution, thereby enhancing fluxes.

The present work concerns hollow fiber configurations that are frequently implemented in PoU systems, due to their relative higher specific membrane filtration area per unit module volume [12]. One experimental study [13] on the use of hollow fiber membranes during gravity driven membrane filtration can be found, reporting the application of hollow fibers in a membrane bioreactor for onsite greywater treatment [13]. The authors observed severe flux decline during one week of operation and stabilizing fluxes within 15 days. The influence of different aeration rates on biological degradation and biomass development was studied to improve wastewater treatment efficiency [13]. Considering fouling development as a temporal phenomenon, understanding the long term effects of the aforementioned factors on fouling becomes essential in order to accurately assess its overall impact on the efficiency of PoU systems. Despite this fact, most studies available in the literature investigate fouling development over short time scales i.e. for periods of 1 h to 24 h. Especially for low pressure filtration, fouling development is slow and a minimum period of 1 week has been shown to stabilize flux rates [14]. The present work hence highlights the fouling behavior in hollow fiber PoU systems operated over longer durations unlike previous studies (>20 days). The specific objectives of the study were to optimize and understand the effects of various operational parameters that affect the fouling development as discussed above, such as intermittent use of the system, inside/out vs. outside/in operation of the hollow fiber configuration, and recirculation of feed water over the membrane surface. These parameters can be useful in designing more efficient hollow fiber based PoU systems. There are only a few studies [3,14,15] addressing fouling under gravity pressures for flat sheet membrane configurations using surface water as feed. We know from literature that membrane geometry and configuration affect fouling development [4]. Hence, in the present work fouling development is studied under gravity pressures using hollow fiber membranes simulating PoU systems. The advantages of low-pressure membrane operation, in this case gravity pressure, are minimal energy consumption since pumping is not required, and almost no manual maintenance. This broadens the applicability of PoU systems.

In the present work we constructed hollow fiber modules to simulate PoU systems for onsite drinking water treatment applications. In the study, we used surface water containing higher natural organic matter and lower biomass content compared to Jabornig et al. [13] as key foulants. Two hollow fiber configurations with 3 different intermittent intervals of operation and the effect of feed recirculation on fouling development were investigated.

2. Experimental section

2.1. Experimental set-up

A schematic representation of the experimental set-up is shown in Fig. 1. A hydrostatic head provides 100 mbar as transmembrane pressure. Each experimental run was duplicated using two identical modules. All the experiments were conducted at 20 ± 2 °C. Intermittent operations were performed using magnetic valves (M&M International, Italy) coupled with automatic timers (Grassini, Germany). The permeate flux was measured manually every day using a graduated cylinder and a stopwatch. At least two measurements were recorded each day and the average value of the flux was considered.

The viscosity was temperature corrected and plugged in expression (1) to calculate the hydraulic resistance using the following equation [12]:

$$R = \frac{TMP}{\eta J_s} \quad (1)$$

where R is the total hydraulic resistance (1/m), TMP is the transmembrane pressure (Pa), η is the dynamic viscosity of the permeate (Pa·s) and J_s is the flux ($m^3/m^2 \cdot s$).

2.2. Membrane modules

Polyethersulphone (PES) inside/out (I/O) hollow fiber membranes (3 mm ID, 4.5 mm OD) with a MWCO of 100–150 kDa were kindly supplied by Pentair X-Flow BV (Enschede, The Netherlands). These I/O hollow fibers were used to construct membrane modules mimicking commercial PoU systems, with a membrane area of 0.15 m^2 (O/I) and 0.07 m^2 (I/O). For module construction, the membranes were stacked inside a PVC housing, and subsequently potted into the housing with an epoxy resin cured overnight. Clean water permeability for these hollow fiber membrane modules ranged from 260 to 400 $L/m^2 \cdot h \cdot bar$.

Flat sheet PES membranes (type UP 150, MWCO 150 kDa) were purchased from Microdyn Nadir (Germany). Its clean water permeability is >286 $L/m^2 \cdot h \cdot bar$ as per manufacturer. Polycarbonate membrane holders (48 mm, Whatman, VWR, The Netherlands) were used for flat sheet experiments (membrane filtration area 0.0018 m^2).

Prior to filtration, all hollow fiber membrane modules were soaked in demi water overnight, and then rinsed once with 20% ethanol and twice with demi water as recommended by the manufacturer to remove conservation agents prior to the filtration experiments. Hollow fiber modules were checked for leakages by an air-leak test before installing them in the experimental set-up. All installed modules were subsequently checked for leakage at the start of each experiment by determining the number of total coliforms in feed and permeate samples, whereby leaking modules (rejection of coliform <100%) were discarded.

2.3. Chemical analyses and feed water characteristics

Surface water from the Potmarge river (Leeuwarden, The Netherlands) was collected once every 2–3 days and used directly. The total carbon, total organic carbon (TOC) and inorganic carbon of feed and permeate were analyzed by a TOC analyzer (Shimadzu Scientific instruments, Kyoto, Japan). Chemical oxygen demand (COD) of feed and permeate were measured daily using a Hach Lange cuvette test kit (LCK 414 effluent 5–60 mg/L). pH and conductivity were measured using portable meters (WTW, Germany). Turbidity was measured using a Hach 2100N-IS Turbidity meter (ISO Method 7027). Dissolved Oxygen (DO) was measured using a DO probe (HQ30d, Hach). Natural Organic Matter (NOM) fractions were analyzed by Liquid Chromatography-Organic Carbon Detection (LC-OCD) with a UV and organic nitrogen detector (OND) attached to it (Model 8, DOC Labor, Germany). NOM comprises of biopolymers, humic acids, low molecular weight acids

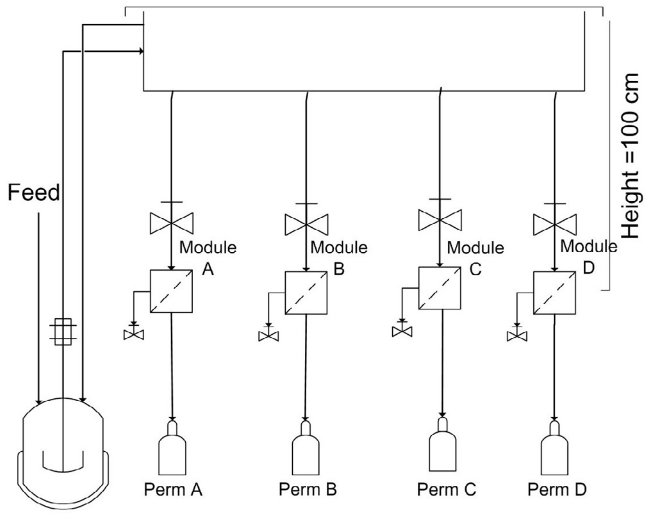

Fig. 1. Experimental scheme of the simulated Point-of-Use (PoU) system showing four modules A-D. Perm (permeate) is collected in flasks as shown in the figure; black lines with arrows indicate direction of the water flow through the set-up.

and neutrals. Separation of NOM fractions in LC-OCD takes place according to their molecular weight cut off (MWCO) on a size exclusion chromatographic column. Larger molecules have the lowest retention time and smaller molecules have the longest retention times. The average raw water characteristics of the Potmarge river water are shown in Table 1.

Total coliform and *E. coli* in feed and permeate samples were determined using the USEPA method 10029 for coliform detection for drinking water applications. m-Coli broth (Hach) was used as medium for incubation. A sample volume of 5 mL was filtered through a sterilized 0.45 μm white gridded filter paper (Pall Life Sciences, The Netherlands). The filter paper was incubated in a sterile petri dish containing adsorbent pads (Pall Life Sciences, The Netherlands) and broth at 35 ± 2 °C for 24 h. The petri dish was placed in an incubator (Innova 42, New Brunswick Scientific). Colony counting was performed the following day at 10× magnification using a Leica MZ9.5 optical microscope. Red colonies were total coliforms, except *E. coli* that appeared as blue colonies.

2.4. Sample preparation and Scanning Electron Microscopy (SEM)

Fixation of membrane samples was done using 2.5% (v/v) glutaraldehyde solution (Sigma–Aldrich, Steinheim, Germany) and incubating them overnight at 4 °C. On the subsequent day, samples were washed with Phosphate-buffered saline (PBS) and dehydrated with ethanol. The washing step was performed three times for 7 min per step with 1X PBS (10 mM), followed by dehydration with 30%, 50%, 70%, and 90% (v/v with Milli-Q) ethanol solutions for 20 min each, and finally twice with 100% ethanol for 30 min each. Milli-Q water (>18 MΩ·cm) used in the experiments was obtained from a Millipore Milli-Q® Biocel with a Q-grade® column. The dehydrated samples were air-dried in a drying chamber overnight at 37 °C (MMM Group, Venticell, Brno, Czech Republic). Finally, the samples were sputtered with gold (Jeol JFC-1200 Fine Coater, Japan) and visualized under an SEM (JSM6480LV microscope, JEOL Technics Ltd., Japan) operated at an accelerating voltage of 6 kV in a high vacuum mode.

2.5. ATP and TOC analysis of the fouling layers

Adenosine triphosphate or ATP gives the measure of living cellular material and in the present study refers to the living biomass within the fouling layer on the membrane surface [16]. For ATP measurements, membrane samples were shaken for 40 min at 1500 rpm (Heidolph MultiReax) in 1X PBS to remove reversible fouling from the surface. Afterwards, the samples were stored in ice and brought immediately to the local water supply company (Vitens, Leeuwarden, The Netherlands) for further analysis. The refrigerated samples were sonicated in an ultrasonic water bath at 37 kHz for 5 min to remove the remaining cells from the membrane surface and subsequently vortexed for a few seconds at a maximum velocity of 2500 rpm. An "ATP Biomass Kit HS" (Biothema, Sweden) with a lysis agent 'Celsis LuminEX' ATP Releasing Agent (Celsis, USA) was used to quantify ATP levels in the samples. The final concentrations were measured using an ATP microplate reader (CentroXS3, Berthold technologies, Germany). The error margin for the ATP measurements reported is 10%.

Membrane samples for TOC analysis were placed in 15 mL centrifuge vials containing 10 mL of Milli-Q water. Next, the samples were treated with an ultrasonic probe (Branson Sonifier 250, G. Heinemann Ultraschall- und Labortechnik, Germany) for 1 min to release all TOC attached to the membrane into the solution. Afterwards, the samples were placed in a TOC free glass vial and an additional 10 mL Milli-Q was added to make up 20 mL of sample volume. TOC was measured using a TOC analyzer, as described previously in Section 2.2. The measurement error for TOC analysis was less than 10%.

Table 1
Potmarge water characteristics used as feed water for the experiments. Values averaged over a period of 30 days.

Parameter	Value	Unit
Total Carbon	55 ± 3	mg/L
Total Organic Carbon	15 ± 3	mg/L
Inorganic Carbon	40 ± 3	mg/L
pH	8.0 ± 0.5	–
Conductivity	790 ± 70	μS/cm
Dissolved Oxygen	8.0 ± 0.5	mg/L
Turbidity	5 ± 3	NTU
Chemical Oxygen Demand	35 ± 3	mg/L
Humic acids	13 ± 3	mg/L
Biopolymers	0.8 ± 0.2	mg/L

2.6. Variables

The effects of module geometry/configuration, feed recirculation and (dis)continuous operation on fouling behavior of the low pressure ultrafiltration PoU systems were investigated. Two types of module configurations i.e. flat sheets and hollow fibers, are compared and results are shown in Section 3.1. PoU systems are usually operated intermittently in real life applications [17,18]; hence 2 different run times (4 h/day and 9 h/day, respectively) were compared to continuous (24 h) hollow fiber membrane operation. In Section 3.2, three modes of intermittent operation were studied on two different flow configurations (O/I and I/O) as shown in Table 2, using Potmarge water (surface water) as feed. Table 2 shows the duration and time intervals for permeate production for different operational conditions; 4/20 for example refers to a feed supply duration of 4 h (from 09:00 to 13:00 h), with a standstill period of 20 h between 13:00 and 09:00 h. In order to study the effect of feed flow on fouling, cross-flow experiments using the hollow fiber configuration were designed wherein the feed stream is recirculated at 1200–1500 mL/min using a peristaltic pump to introduce shear stress (around 9×10^{-4} Pa along the walls of the hollow fibers) on the membrane surface. A large feed tank volume ensured there was no change in composition of feed when recycling the feed stream. Reynolds number was calculated to be

Table 2
Four different intermittent time intervals are shown using Potmarge water as feed for both O/I and I/O membrane configurations.

	Operational condition	Feed ON (h)	Feed OFF (h)	Permeation ON, (h)	Permeation OFF, (h)
1	4/20	4	20	09:00–13:00	13:00–09:00
2	2/5/2/15	4	20	09:00–11:00; 16:00–18:00	11:00–16:00; 18:00–09:00
3	9/15	9	15	09:00–18:00	18:00–09:00
4	24/0	24	0	09:00–09:00	0

around 400 inside the module around the hollow fibers. The results are presented in Section 3.3.

3. Results and discussion

3.1. Module configuration and feed water

To address the influence of membrane module configuration on the flux behavior, two different membrane configurations i.e. hollow fiber and flat sheet type were assessed in terms of permeate production and hydraulic resistance. Both modules were operated in dead-end mode; the hollow fiber module was tested in outside/in mode. Fig. 2 illustrates the variation of flux and hydraulic resistance as a function of time, for both configurations. The results correspond to an operational duration of 30 days. Both configurations exhibit qualitatively similar trends. During the first few days of filtration the flux values show a steady drop: a ~4 fold decrease for the hollow fiber configuration and a ~2 fold decrease for the flat sheet configuration. Over longer durations the rate of flux change gradually declines, eventually achieving a constant flux level indicated by the plateau region extending until the end of the experimental run (Fig. 2). As expected, the hydraulic resistance values display exactly opposite trends with respect to the flux variation. Interestingly, quantitative comparison between the hydraulic resistance values of the flat sheet and hollow fiber during the first 4 days of filtration reveals approx. 5 times higher values in case of the flat sheet configuration. Moreover, the rate of flux decline is considerably higher for the hollow fiber in comparison with the flat sheet membrane. Such deviations are most likely attributed to different flow dynamics and hence fouling mechanisms prevalent in the two configurations.

The time dependent flux variation during membrane filtration can be physically classified into three stages: a) initial foulant adsorption and deposition, b) pore constriction and blockage and c) cake or gel layer formation [12,19]. In case of the hollow fiber configuration, it is suggested that the high volumetric permeate flows during the first 24 h accelerates solute transport to the membrane surface. High solute deposition and adsorption rates in turn rapidly clog the membrane pores, leading to a sharp initial decrease in permeate flow rates and a transition into a more gradual decline during intermediate stages. While the sharp decline observed in the beginning is attributed to an internal pore blocking mechanism, the intermediate stage is dominated by deposition and accumulation of foulants. Flow rates continue to decline until the rate of deposition and accumulation of foulants is equilibrated by back diffusion and re-dissolution of foulants [15]. This appears as a plateau in the flux and hydraulic resistance trends (Fig. 2).

Initial permeate flows in the flat sheet configuration displayed significantly lower values in comparison to the hollow fiber membranes (Fig. 2a). Contrary to the steep drop observed in the flux values for hollow fiber configuration, the rate of flux decline was much slower and more steady during the flat sheet membrane filtration. More gradual flux decline in the flat sheet configuration suggests fouling development to take place by formation of a cake layer, which thickens over time and restricts the membrane permeability.

The type of fouling mechanisms i.e. pore blocking and/or cake formation in ultrafiltration as also observed in the present study primarily depends upon pore size distribution and pore structure [20], foulant composition and concentration in the feed water [15], operational conditions and membrane material. Since the same feed was fed to both configurations in our study, it is likely that the pore structure of the membranes determines the mode of fouling. In this respect, the hollow fiber membranes starting at a higher initial flux are assumed to comprise of larger and more open pores that suffer from severe pore blocking within the first week of operation. On the other hand, the flat sheet configuration displaying lower initial fluxes and a steady decrease in flow rates tend to foul by formation of a cake layer.

Depending upon the type of feed and the MWCO of membranes used, the composition of the cake layer can be either dominated by inorganics or natural organic matter (NOM) molecules [7,21,22]. In this study, one of the major components of fouling layer based on retained fractions of NOM are biopolymers, and to some extent humic acids, as these were the only measurable dissolved organic carbon (DOC) fractions (as calculated from the difference in feed and permeate concentrations). Fig. 3 shows the overall retention of biopolymers and humic acids after 30 days of filtration for both hollow fiber and flat sheet membranes. Macromolecules, such as biopolymers, are known to cause severe fouling during low pressure ultrafiltration [23–26]. In the present study, we used open and low pressure ultrafiltration membranes, hence it was observed that the cake layer comprised of mainly biopolymers and a small fraction of humic acids. Besides NOM fractions, feed and permeate analysis of inorganic carbon and ions (Si, Ca, Na, Mg, K, Fe, P) showed negligible retention of inorganics on the membrane surface. To conclude, both hollow fiber and flat sheet membranes suffered from mainly NOM fouling, specifically biopolymers.

3.2. Operational modes and discontinuous operation

The influence of mode of operation on fouling development was investigated by operating the systems intermittently vis-à-vis continuously. Four different modes were investigated, as summarized in Table 2. All three intermittent systems were turned on/off exactly at the same time every day using automatic timers and magnetic valves (described in Section 2.1). Two different operational modes were employed for all intermittent operations: O/I and I/O mode. Fig. 4 graphically represents the hydraulic resistances at the end of the run for each operational mode. The corresponding fluxes for two different operational modes with their respective operational time intervals (in hours, given in brackets) are as follows a) for O/I mode 1) 3.6 $L/m^2{\cdot}h$ (4 ON/20 OFF) 2) 2.7 $L/m^2{\cdot}h$ (2 ON/5 OFF/2 ON/15 OFF) 3) 2.5 $L/m^2{\cdot}h$ (9 ON/15 OFF) 4) 1.6 $L/m^2{\cdot}h$ (24 ON/0 OFF) b) for I/O mode 1) 20.2 $L/m^2{\cdot}h$ (4 ON/20 OFF) 2) 22.7 $L/m^2{\cdot}h$ (2 ON/5 OFF/2 ON/15 OFF) 3) 13.6 $L/m^2{\cdot}h$ (9 ON/15 OFF) 4) 2.8 $L/m^2{\cdot}h$ (24 ON/0 OFF). The trends evince a significant lower hydraulic resistance when membranes are operated intermittently in contrast to the continuous mode.

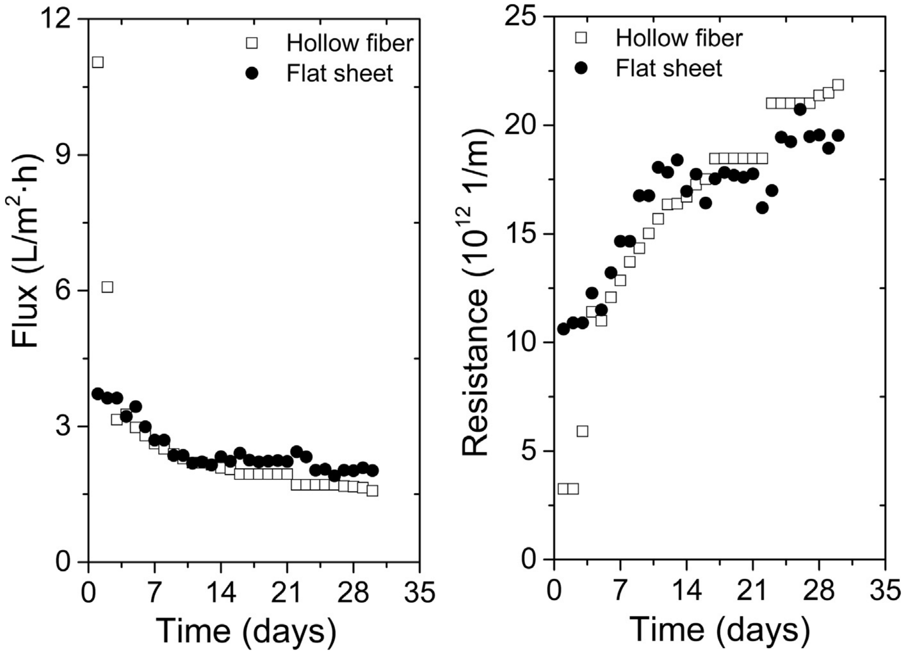

Fig. 2. Flux data (a) and hydraulic resistance (b) of hollow fiber (O/I) and flat sheet membrane configurations using Potmarge (surface) water as feed for an operational run of 30 days.

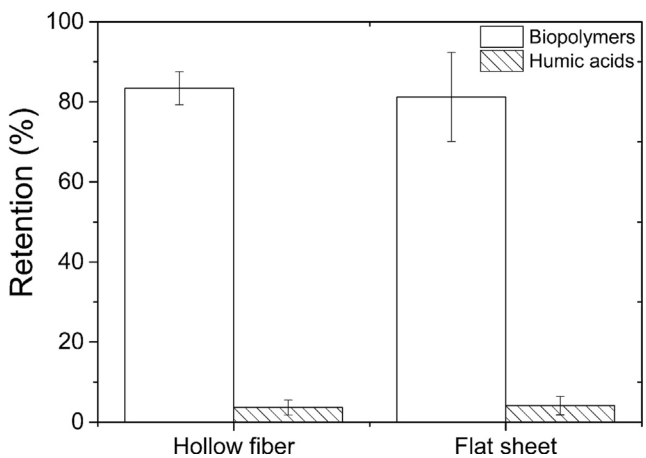

Fig. 3. Biopolymer retention and humic acids retention for hollow fiber and flat sheet membrane filtration after an experimental run of 30 days using Potmarge surface water as feed.

Furthermore, the O/I operational mode results in overall higher hydraulic resistance than the I/O mode.

The accumulated DOC on the membrane surface for intermittently and continuously operated membrane systems is shown in Fig. 5. An important factor for intermittent operations is the lower foulant load delivered per unit membrane area due to discontinuous use of the system (Fig. 5) and lower permeate production capacity than a continuous system. It is observed that although an intermittent system has 1/6th of permeate production compared to a continuous system, the accumulated DOC for intermittent system is half of the continuous system. Hence, a significant portion of the fouling is not permeation related. The effects of intermittent operation on drinking water production are reported in literature for slow sand filtration [18,27] and membrane filtration based PoU systems [3]. A secondary effect of intermittent operation is the relaxation of the fouling layer during standstill periods. It has been shown that absence of permeate flow for a defined time interval leads to relaxation of the fouling layer deposited on the membrane surface [28–30]. Hong et al. [31] showed that relaxation of the fouling layer can lead to 100% flux recovery in a membrane bioreactor. During such standstill periods when the fouling layer relaxes, it is assumed that reversibly bound particles diffuse away from the membrane surface to the bulk fluid [31]. This further leads to a lower hydraulic resistance of the accumulated fouling layer and correspondingly higher fluxes.

Comparing the inside/out (I/O) operational mode with the outside/in (O/I) mode, we observe that the hydraulic resistances of I/O systems are much lower than those of O/I systems. Fig. 4 also shows that intermittently operated O/I systems (4/20, 2/5/2/15, and 9/15 in Fig. 4) show similar hydraulic resistances as observed for the continuously operated I/O system (24). It is important to stress that the same membranes were used in both I/O as well as in the O/I configurations and the same membrane area was assumed for both. Membrane permeability is dependent upon the internal pore structure of the membranes, which in this case is asymmetric with the larger pores being on the outside and the separation layer on the inside. As the location of the fouling layer is not known, this may affect the effective membrane area as well. Initial permeation rates are crucial in determining the extent and type of fouling mechanism occurring at the beginning of the filtration process, which plays a critical role in defining the severity of flux decline [30]. Pore blocking/constriction occurs due to accumulation of foulants within the internal structure of membrane whereas cake layer forms on the membrane surface. During O/I operation pore blocking/constriction is assumed to be the first fouling mechanism to evolve. Cake layer formation leads to severe flux decline and fouling on the membrane surface during I/O operation, as illustrated in Fig. 6. Varying fouling mechanisms such as pore constriction followed by severe pore blocking and cake layer formation in the O/I operational mode lead to larger hydraulic resistances compared to I/O operated membrane modules. Fig. 6c and d show the cake layer formation on the inside membrane surface of the I/O operated module. On the other hand, Fig. 6e and f reveal extensive pore blocking/constriction on the outside membrane surface of the O/I operated membrane module.

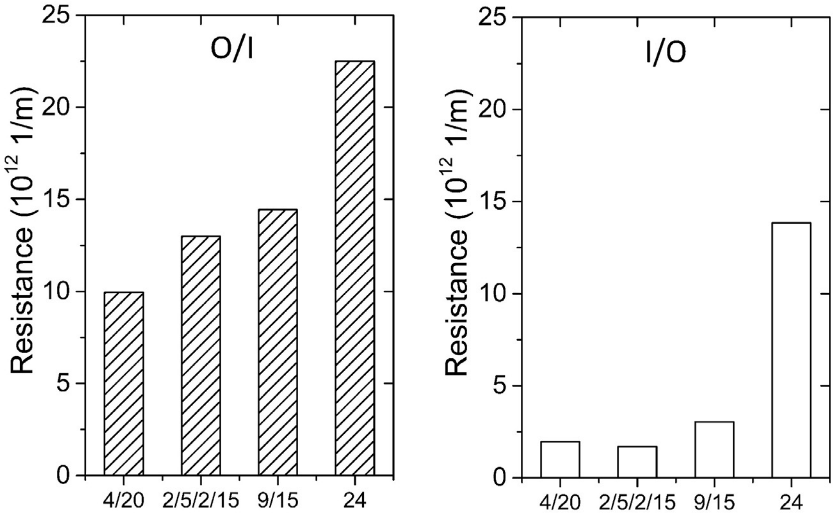

Fig. 4. Hydraulic resistances at the end of the experimental runs (26 days) for outside/in (O/I) (left) and inside/out (I/O) (right) configurations at 4 different operational conditions a) 4 h ON/20 h OFF b) 2 h On/5 h OFF/2 h ON/15 h OFF c) 9 h ON/15 h OFF d) 24 h ON. In all cases, Potmarge surface water was used as feed.

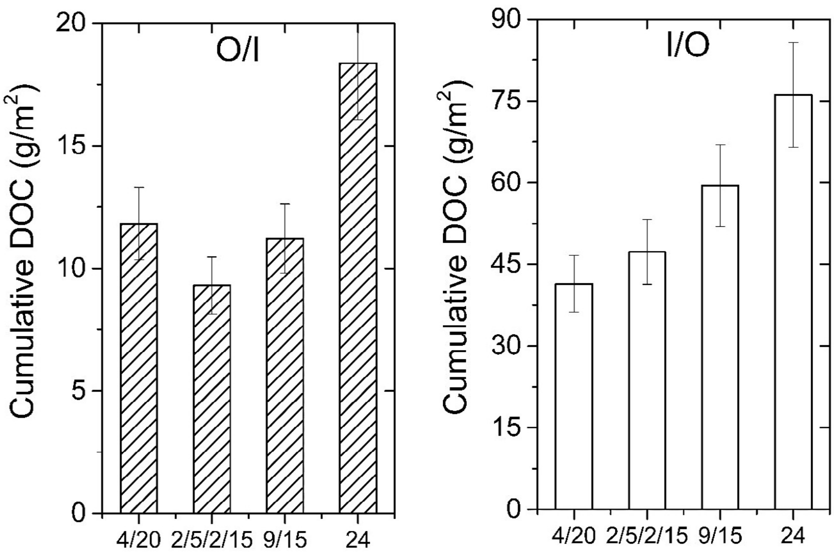

Fig. 5. Cumulative DOC (Dissolved Organic Carbon) at the end of the experimental runs (26 days) for outside/in (O/I) and inside/out (I/O) configurations at 4 different operational conditions a) 4 h ON/20 h OFF b) 2 h On/5 h OFF/2 h ON/15 h OFF c) 9 h ON/15 h OFF d) 24 h ON. In all cases, Potmarge surface water was used as feed.

Similar findings are reported in literature [6], wherein it was observed that pore blocking leads to higher flux decline compared to cake layer formation. Additionally, physical cleaning was found to be more effective for recovering fluxes when the membranes were fouled by cake layer formation compared to internal pore blocking [6].

Fig. 7 shows the accumulated ATP and TOC amounts on the membrane surface for two different operational modes (O/I and I/O). A high standard deviation is reported for ATP measurements due to non-homogeneous deposition of retained solute on the membrane surface. Hence, the membrane coupons belonging to the same module have a great variability in ATP biomass. The non-homogeneous distribution of foulants can be visually observed in the SEM pictures shown in Fig. 6. Generally, the O/I modes revealed a higher amount of ATP on their surfaces (50–80 $\mu g/m^2$) compared to the I/O systems (10–30 $\mu g/m^2$). A suggestive explanation for higher ATP in the case of O/I operational mode could be the presence of bigger pores on the outer surface that can potentially allow small bacteria and living organisms to access the internal membrane structure, thereby contributing to higher ATP accumulation. In contrast, the I/O operational mode retains most of the living biomass on the surface itself. In contrast, TOC for the I/O operational modes was always higher than that for the O/I operational modes, as shown in Fig. 7. In the I/O operational mode the foulants remain confined inside the lumen of the hollow fiber membrane. On the other hand, the O/I operational mode has a stagnant volume around the fibers that keeps the foulants in suspension [32]. Hence, less organic matter is deposited on the membrane surface in the O/I systems resulting in a lower TOC amount accumulated per unit membrane area.

3.3. Cross-flow effects

Cross-flow or recirculation of feed over the membrane surface was introduced in order to understand its role on fouling. Membrane modules in O/I operational mode were simultaneously

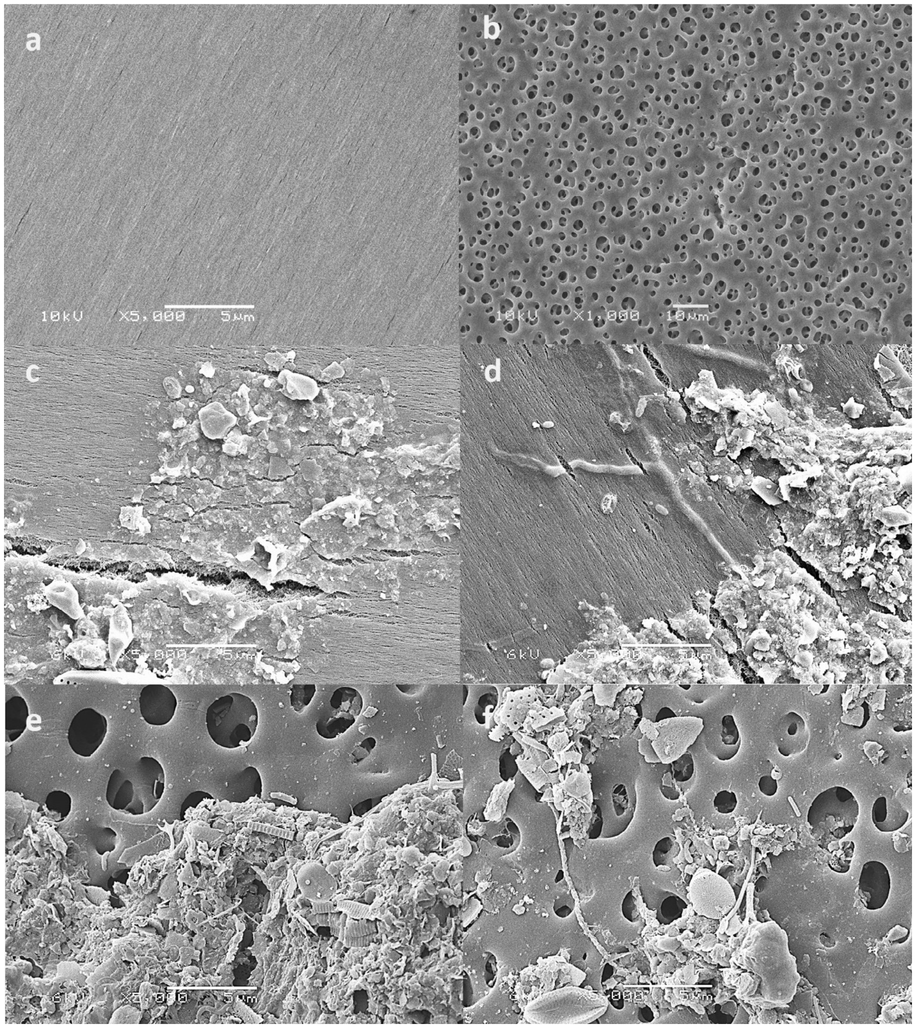

Fig. 6. SEM images of (a) clean hollow fiber membrane surface, inside at 5000×, (b) outside at 1000×, (c,d) inside of a fouled inside/out (I/O) operated hollow fiber membrane at 5000×, and (e,f) the outside of a fouled outside/in (O/I) operated hollow fiber membrane at 5000×.

operated in four different modes: 1) a "continuous" dead-end operation as reference for 24 h/day; 2) an "intermittent" system, operated intermittently in dead end mode for 9 h/day followed by 15 h off/day (no feed supply); 3) a "continuous + cross flow" system with recirculation of the feed operated continuously 24 h/day, and 4) "intermittent + cross flow" with recirculation of the feed and operated intermittently for 9 h/day followed by 15 h/day without feed supply.

For all operational modes, a sharp decline in flux was observed, similar to the trends shown in Section 3.1. The final stabilized permeate fluxes were around 2 ± 1 L/m^2·h under all experimental conditions. Fig. 8 shows the hydraulic resistances as a function of the cumulative permeate production volumes for the four different O/I operational modes. Initially at a given hydraulic resistance, intermittent modules (intermittent and intermittent + cross flow) reveal a lower production capacity due to shorter operational time periods compared to the continuous systems (continuous and continuous + cross flow). At the end of the 40 days experimental run, continuous systems had produced around 550–600 L of permeate ending up in slightly higher hydraulic resistances in comparison with intermittent systems that produced 400–450 L of permeate. Though the amount of water filtered through all the four systems varies, we observe comparable resistances for all systems. Within the accuracy of experiments, no significant differences are observed in resistance growth and at end of the run, all the four systems approach the stabilization stage (Fig. 8).

At the end of the experimental run, membranes were autopsied for TOC and ATP analysis. TOC accumulated on the membrane surface in modules without crossflow was 120 mg/m^2 for a continuous system and 20 mg/m^2 for an intermittent system. On the other hand, TOC accumulated on the membrane surface in modules with cross flow was 70 mg/m^2 for the continuous system and 60 mg/m^2 for the intermittent system. The continuously operated system showed higher accumulated TOC compared to the intermittent and cross flow systems. Cross flows lead to shear stress on the bacterial biomass. According to literature, shear stresses are known to enhance microbial growth in biological systems [33]. ATP accumulated on the membrane in a module without cross-flow was 7.5 µg/m^2 for the continuous and 5 µg/m^2 for the intermittent system without crossflow. ATP accumulated on the membrane surface in the modules with cross-flow was 13 µg/m^2 for continuous and 12 µg/m^2 for intermittent operation. The data shows that applying a crossflow led to two times higher ATP content accumulated on the membrane surface. However, the higher ATP content (living biomass) is assumed not to have a large influence on the fouling layer as the hydraulic resistances for continuous systems with and without crossflow are similar (Fig. 8).

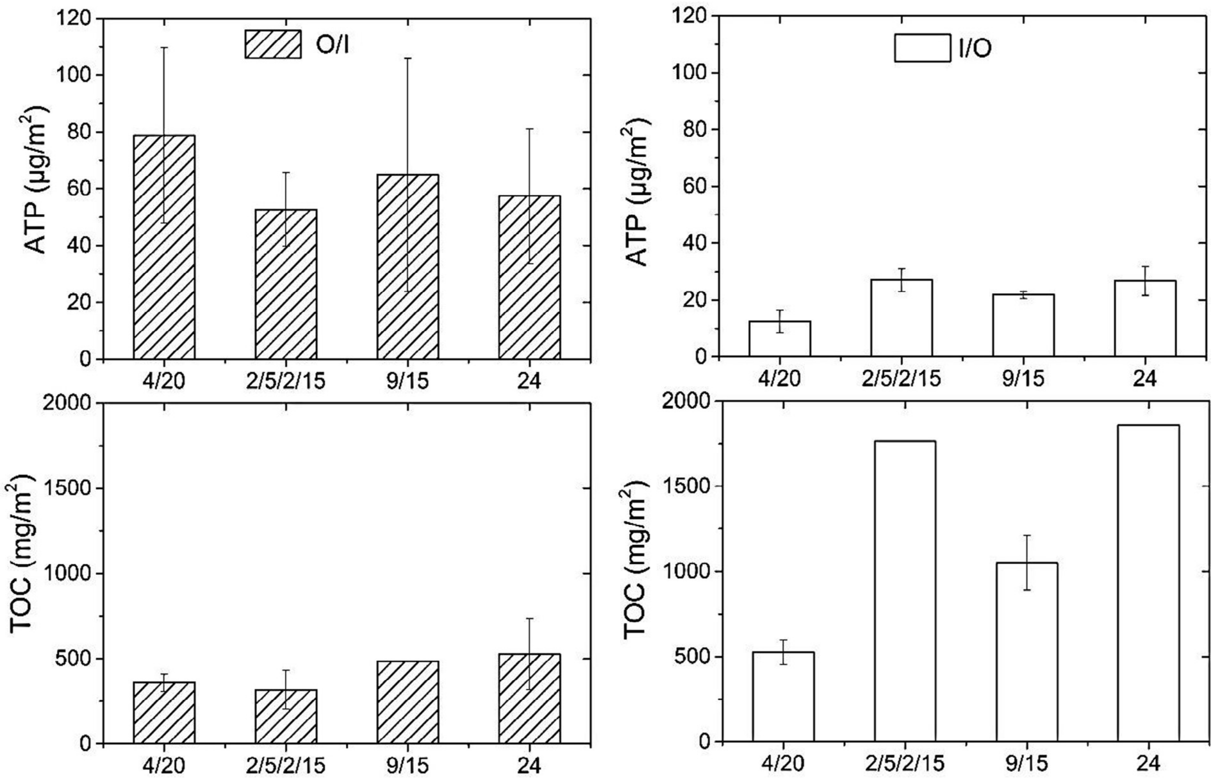

Fig. 7. ATP and TOC values at the end of the experimental runs (26 days) for outside/in (O/I) and inside/out (I/O) configurations at 4 different operational conditions a) 4 h ON/20 h OFF b) 2 h On/5 h OFF/2 h ON/15 h OFF c) 9 h ON/15 h OFF d) 24 h ON. Potmarge surface water was used as feed.

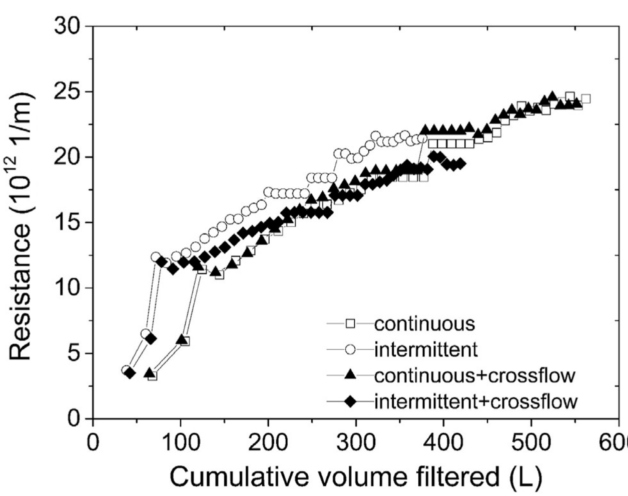

Fig. 8. Hydraulic resistance versus cumulative permeate volume filtered during 40 days of O/I operation under four different conditions: dead end continuous, 24 h ON ('continuous'); intermittent, 9 h ON/15 h OFF ('intermittent'); continuous operation with crossflow with recirculation of feed, 24 h ON ('continuous + cross flow') and intermittent operation with crossflow with recirculation of feed, 9 h ON/15 h OFF ('intermittent + cross flow), all using Potmarge surface water as feed.

4. Conclusions

In the present study various operational conditions affecting permeate production and fouling development on membranes in a PoU system, such as flat sheets vs hollow fiber membrane configuration, intermittent vs. continuous operation, inside/out vs. outside/in configuration, and cross-flow pattern were investigated. Additionally, the phenomenon of flux stabilization was extended to hollow fiber membrane filtration based home-made PoU systems.

From the experiments it can be concluded that pore blocking initiates the fouling in the hollow fiber membranes studied followed by cake layer formation, whereas fouling begins with a cake layer for the flat sheet membrane configuration tested. Hence, a sharp flux decline is observed in the former case compared to the latter. Cake layer formation is the main fouling mechanism for inside/out operation, and pore blocking dominates the outside/in membrane configuration operated systems using a hollow fiber asymmetric membrane with the denser (separating) layer on the inside. The fouling layer comprises of mainly biopolymers and humic acids. The intermittent inside/out configuration results in lower hydraulic resistances compared to outside/in due to lower foulant load per unit membrane area and relaxation of fouling layer.

Based on these results, either forward or backward flush as a cleaning strategy is recommended as it can greatly enhance the operational time period of a PoU device based on membrane filtration system operated under gravity pressures. Hence, best operating conditions for water purification for given conditions as in the present study in terms of feed water and operating pressure are inside/out mode operated intermittently, combined with flushing.

Acknowledgements

This work was performed in the cooperation framework of Wetsus, European Centre of Excellence for Sustainable Water Technology (www.wetsus.nl). Wetsus is co-funded by the Dutch Ministry of Economic Affairs and Ministry of Infrastructure and Environment, the European Union Regional Development Fund, the Province of Fryslân, and the Northern Netherlands Provinces. The authors would like to extend gratitude to the entire Biofouling theme of Wetsus for the fruitful discussions and their financial support.

Appendix

Cost estimation of a PoU system

The drinking water costs per liter of produced potable water of a PoU system include both initial investment costs (CAPEX) and cost of utilities (energy and cleaning; OPEX). The World Health Organization categorizes costs of PoU systems as low (US$ 10), moderate (US$ 10–100) and high (>US$ 100), [34,35]. The price of water produced per unit total costs is primarily affected by three parameters a) permeate production capacity of the system, b) the lifetime of the membrane and c) the initial module cost [36].

According to the WHO, per capita water requirements for survival and cooking needs in an emergency have been estimated to be between 5 and 9 L/day, and including hygiene practices it increases to 7.5–15 L/day [37]. A household of 5 family members would therefore need a minimum of 37.5 L to fulfill their daily water demands. Initial investment for membrane filtration includes both required membrane material costs and module construction costs. The price of a hollow fiber UF membrane module for water treatment is around 10–40 €/m^2 [32] sustaining a designed flux of 10 L/m^2·h that decreases to 2 L/m^2·h as seen in the present study (using a very challenging water stream). The required membrane module costs can hence be calculated by the following expression,

$$\text{Required membrane module costs} = \frac{\text{DWC}}{\text{Permeate Flux}} \times \text{Membrane module cost} \tag{A.1}$$

where DWC is daily water consumption per household. Substituting the aforementioned values of DWC as 37 L/day/household, an average flux of 6 L/m^2·h and an average module costs of 25 €/m^2 in Eq (3), membrane module costs would be in the range of 1–10 €. On the basis of the above calculations, the overall annual investment costs associated with initial set-up of a PoU system can be estimated to be less than 9 € (equivalent to 10 USD as on 8 Feb 2016). It is to be mentioned that the calculations neglect costs associated with utilities since the estimates are provided for a gravity driven filtration system with no pumping requirements. This suggests that PoU systems manufactured on the basis of current findings can potentially meet the requirements of safe, clean and low cost drinking water.

References

[1] Results of WHO survey on demand for testing in WHO Scheme to Evaluate Household Water Treatment Technologies, World Health Organization, Geneva, Switzerland, 2014.

[2] M.J. Pryor, E.P. Jacobs, J.P. Botes, V.L. Pillay, A low pressure ultrafiltration membrane system for potable water supply to developing communities in South Africa, Desalination 119 (1998) 103–111.

[3] M. Peter-Varbanets, W. Gujer, W. Pronk, Intermittent operation of ultra-low pressure ultrafiltration for decentralized drinking water treatment, Water Res. 46 (2012) 3272–3282.

[4] J.N. Ghogomu, C. Guigui, J.C. Rouch, M.J. Clifton, P. Aptel, Hollow-fibre membrane module design: comparison of different curved geometries with Dean vortices, J. Membr. Sci. 181 (2001) 71–80.

[5] N. Shamsuddin, D.B. Das, V.M. Starov, Filtration of natural organic matter using ultrafiltration membranes for drinking water purposes: Circular cross-flow compared with stirred dead end flow, Chem. Eng. J. 276 (2015) 331–339.

[6] F.I. Hai, K. Yamamoto, K. Fukushi, Different fouling modes of submerged hollow-fiber and flat-sheet membranes induced by high strength wastewater with concurrent biofouling, Desalination 180 (2005) 89–97.

[7] G. Amy, Fundamental understanding of organic matter fouling of membranes, Desalination 231 (2008) 44–51.

[8] R. Bian, K. Yamamoto, Y. Watanabe, Effect of shear rate on controlling the concentration polarization and membrane fouling, Desalination 131 (2000) 225–236.

[9] S. Lee, C.H. Lee, Effect of operating conditions on CaSO4 scale formation mechanism in nanofiltration for water softening, Water Res. 34 (2000) 3854–3866.

[10] S. Bhattacharjee, G.M. Johnston, A model of membrane fouling by salt precipitation from multicomponent ionic mixtures in crossflow nanofiltration, Environ. Eng. Sci. 19 (2002) 399–412.

[11] H. Choi, K. Zhang, D.D. Dionysiou, D.B. Oerther, G.A. Sorial, Influence of cross-flow velocity on membrane performance during filtration of biological suspension, J. Membr. Sci. 248 (2005) 189–199.

[12] M. Mulder, Basic Principles of Membrane Technology, second ed., Kluwer Academic Publisher, The Netherlands, 1996.

[13] S. Jabornig, S.M. Podmirseg, A novel fixed fibre biofilm membrane process for on-site greywater reclamation requiring no fouling control, Biotechnol. Bioeng. 112 (2015) 484–493.

[14] M. Peter-Varbanets, F. Hammes, M. Vital, W. Pronk, Stabilization of flux during dead-end ultra-low pressure ultrafiltration, Water Res. 44 (2010) 3607–3616.

[15] M. Peter-Varbanets, J. Margot, J. Traber, W. Pronk, Mechanisms of membrane fouling during ultra-low pressure ultrafiltration, J. Membr. Sci. 377 (2011) 42–53.

[16] O. Holm-Hansen, The Use of ATP Determinations in Ecological Studies, Bull. Ecol. Res. Committee (1973) 215–222.

[17] A. Schäfer, A. Broeckmann, B. Richards, Renewable energy powered membrane technology. 1. Development and characterization of a photovoltaic hybrid membrane system, Environ. Sci. Technol. 41 (2007) 998–1003.

[18] S.-S.K. Tiwari, W.-P. Schmidt, J. Darby, Z.G. Kariuki, M.W. Jenkins, Intermittent slow sand filtration for preventing diarrhoea among children in Kenyan households using unimproved water sources: randomized controlled trial, Tropical Med. Int. Health 14 (2009) 1374–1382.

[19] A.R. Costa, M.N. de Pinho, M. Elimelech, Mechanisms of colloidal natural organic matter fouling in ultrafiltration, J. Membr. Sci. 281 (2006) 716–725.

[20] F. Wang, V.V. Tarabara, Pore blocking mechanisms during early stages of membrane fouling by colloids, J. Colloid Interface Sci. 328 (2008) 464–469.

[21] Y. Ye, P. Le Clech, V. Chen, A.G. Fane, B. Jefferson, Fouling mechanisms of alginate solutions as model extracellular polymeric substances, Desalination 175 (2005) 7–20.

[22] L. Ji, J. Zhou, Influence of aeration on microbial polymers and membrane fouling in submerged membrane bioreactors, J. Membr. Sci. 276 (2006) 168–177.

[23] W.R. Bowen, F. Jenner, Theoretical descriptions of membrane filtration of colloids and fine particles: An assessment and review, Adv. Colloid Interface Sci. 56 (1995) 141–200.

[24] J. Haberkamp, M. Ernst, U. Böckelmann, U. Szewzyk, M. Jekel, Complexity of ultrafiltration membrane fouling caused by macromolecular dissolved organic compounds in secondary effluents, Water Res. 42 (2008) 3153–3161.

[25] M.D. Kennedy, F.P. Muñoz Tobar, G. Amy, J.C. Schippers, Transparent exopolymer particle (TEP) fouling of ultrafiltration membrane systems, Desalin. Water Treat. 6 (2009) 169–176.

[26] X. Zheng, M. Ernst, P.M. Huck, M. Jekel, Biopolymer fouling in dead-end ultrafiltration of treated domestic wastewater, Water Res. 44 (2010) 5212–5221.

[27] M. Elliott, C. Stauber, F. Koksal, F. DiGiano, M. Sobsey, Reductions of E. coli echovirus type 12 and bacteriophages in an intermittently operated household-scale slow sand filter, Water Res. 42 (2008) 2662–2670.

[28] P. van der Marel, A. Zwijnenburg, A. Kemperman, M. Wessling, H. Temmink, W. van der Meer, An improved flux-step method to determine the critical flux and the critical flux for irreversibility in a membrane bioreactor, J. Membr. Sci. 332 (2009) 24–29.

[29] S.P. Hong, T.H. Bae, T.M. Tak, S. Hong, A. Randall, Fouling control in activated sludge submerged hollow fiber membrane bioreactors, Desalination 143 (2002) 219–228.

[30] U. Metzger, P. Le-Clech, R.M. Stuetz, F.H. Frimmel, V. Chen, Characterisation of polymeric fouling in membrane bioreactors and the effect of different filtration modes, J. Membr. Sci. 301 (2007) 180–189.

[31] S. Hong, R.S. Faibish, M. Elimelech, Kinetics of permeate flux decline in crossflow membrane filtration of colloidal suspensions, J. Colloid Interface Sci. 196 (1997) 267–277.

[32] R.W. Baker, Membrane Technology, Wiley Online Library, 2000.

[33] M. Van Loosdrecht, D. Eikelboom, A. Gjaltema, A. Mulder, L. Tijhuis, J. Heijnen, Biofilm structures, Water Sci. Technol. 32 (1995) 35–43.

[34] M. Peter-Varbanets, C. Zurbrügg, C. Swartz, W. Pronk, Decentralized systems for potable water and the potential of membrane technology, Water Res. 43 (2009) 245–265.

[35] D.-G. Kim, H. Kang, S. Han, J.-C. Lee, The increase of antifouling properties of ultrafiltration membrane coated by star-shaped polymers, J. Mater. Chem. 22 (2012) 8654–8661.

[36] S. Kumar, A. Groth, L. Vlacic, An analytical index for evaluating manufacturing cost and performance of low-pressure hollow fibre membrane systems, Desalination 332 (2014) 44–51.

[37] J.R. Du, S. Peldszus, P.M. Huck, X. Feng, Modification of poly(vinylidene fluoride) ultrafiltration membranes with poly(vinyl alcohol) for fouling control in drinking water treatment, Water Res. 43 (2009) 4559–4568.